Constraining Southern Ocean CO2 Flux Uncertainty Using Uncrewed Surface Vehicle Observations

Adrienne J. Sutton[1], Nancy Louise Williams[2], and Bronte David Tilbrook[3]

[1]NOAA Pacific Marine Environmental Laboratory
[2]University of South Florida
[3]CSIRO/ACE CRC

November 23, 2022

Abstract

Remote, harsh conditions of the Southern Ocean challenge our ability to observe the region's influence on the climate system. Southern Ocean air-sea CO2 flux estimates have significant uncertainty due to the reliance on limited ship-dependent observations in combination with satellite-based and interpolated data products. We utilize a new approach, making direct measurements of air-sea CO2, wind speed, and surface ocean properties on an Uncrewed Surface Vehicle (USV). In 2019 the USV completed the first autonomous circumnavigation of Antarctica providing hourly CO2 flux estimates. Using this unique data set to constrain potential error in different measurements and propagate those through the CO2 flux calculation, we find that different wind speed products and sampling frequencies have the largest impact on CO2 flux estimates with biases that range from -4% to +20%. These biases and poorly-constrained interannual variability could account for discrepancies between different approaches to estimating Southern Ocean CO2 uptake.

Constraining Southern Ocean CO_2 Flux Uncertainty Using Uncrewed Surface Vehicle Observations

A. J. Sutton[1], N. L. Williams[2], and B. Tilbrook[3,4]

[1]Pacific Marine Environmental Laboratory, National Oceanic and Atmospheric Administration, Seattle, Washington, USA.

[2]University of South Florida, St. Petersburg, Florida, USA.

[3]Oceans and Atmosphere, Commonwealth Scientific and Industrial Research Organisation, Hobart, Tasmania, Australia.

[4]Australian Antarctic Program Partnership, University of Tasmania, Hobart, Australia.

Corresponding author: Adrienne Sutton (adrienne.sutton@noaa.gov)

Key Points:

- The first autonomous circumnavigation of Antarctica allowed for direct measurements of air-sea CO_2 and wind speed in the Southern Ocean.
- Bias and error propagation of various approaches to calculating CO_2 flux could explain some of the discrepancies between previous estimates.
- Interannual variability that is poorly-constrained by observations are also likely contributing to the discrepancies in CO_2 flux estimates.

Abstract

Remote, harsh conditions of the Southern Ocean challenge our ability to observe the region's influence on the climate system. Southern Ocean air-sea CO_2 flux estimates have significant uncertainty due to the reliance on limited ship-dependent observations in combination with satellite-based and interpolated data products. We utilize a new approach, making direct measurements of air-sea CO_2, wind speed, and surface ocean properties on an Uncrewed Surface Vehicle (USV). In 2019 the USV completed the first autonomous circumnavigation of Antarctica providing hourly CO_2 flux estimates. Using this unique data set to constrain potential error in different measurements and propagate those through the CO_2 flux calculation, we find that different wind speed products and sampling frequencies have the largest impact on CO_2 flux estimates with biases that range from -4% to +20%. These biases and poorly-constrained interannual variability could account for discrepancies between different approaches to estimating Southern Ocean CO_2 uptake.

Plain Language Summary

The Southern Ocean is an important part of the global climate, playing an outsized role in the uptake of heat and carbon. Yet observing the Southern Ocean is challenging due to its size, remoteness, and harsh conditions. In 2019 we completed the first autonomous circumnavigation of Antarctica with an Uncrewed Surface Vehicle (USV), also known as an ocean robot, in order to address some of these observing challenges. By directly measuring air and surface seawater carbon dioxide (CO_2) and wind speed on the USV, we were able to observe CO_2 exchange between the ocean and atmosphere every hour during the mission. Using this data set, we estimated potential errors in these measurements as well as other approaches to estimating CO_2 exchange. The use of different satellite-based wind products and sampling frequency play the largest role in uncertainty of the uptake of CO_2 in the Southern Ocean. In order to reduce this uncertainty and provide a better understanding of the Southern Ocean, expansion of an observing network made up of ships, USVs, and other autonomous devices is necessary.

1 Introduction

Covering only 30% of the global ocean surface, the Southern Ocean (most often defined as south of 30–35°S) plays an outsized role in the climate system. It is the meeting point of ocean currents and a connector between the atmosphere and ocean interior for the transfer of heat and carbon, accounting for as much as 75% and 40% of global ocean heat and carbon uptake, respectively (Frölicher et al., 2014; Khatiwala et al., 2009). While questions remain as to all of the mechanisms that contribute to CO_2 flux and the overturning circulation in the Southern Ocean, it is becoming clear that control of net CO_2 uptake over annual to decadal scales is dominated by wind-driven physical mixing and upwelling of carbon-rich deep water (Iudicone et al., 2011; Lovenduski et al., 2008).

Southern Ocean CO_2 flux is primarily a balance between the outgassing of natural carbon in upwelled waters not taken up by biological processes and the flux of anthropogenic carbon into the ocean driven by increasing atmospheric CO_2. These processes occur continuously and simultaneously as cold, carbon-rich water outgasses in upwelling regimes, and absorbs anthropogenic heat and carbon as the water flows north in the surface layer to warmer regimes. These processes vary across the diversity of Southern Ocean regimes from the temperature-dominated system in the Subtropical Zone to the sea ice- and biologically-dominated regime closest to Antarctica.

The combination of these diverse and variable biogeochemical regimes, sparse observations, and inadequate constraint of circulation in models challenge estimates of Southern Ocean CO_2 uptake. Climatological mean uptake estimates based on observations from ships range from -0.8 to -1.0 Pg C yr^{-1} (Landschützer et al., 2014; Takahashi et al., 2009). While the magnitude of interannual variability is unknown, the temporal variability of CO_2 flux at interannual to decadal time scales is correlated with atmospheric variability as defined by the Southern Annular Mode (SAM) index: the difference in mean sea level pressure between 40°S and 65°S (Marshall, 2003). When the SAM index is positive, winds south of 45°S increase, potentially accelerating upwelling of carbon-rich deep water and reducing net CO_2 uptake. A negative SAM index is associated with a reduction of both upwelling and ventilation of CO_2 to the atmosphere, allowing increased net CO_2 uptake. However, there are regional variations in CO_2 flux response to SAM conditions that are not fully understood (Keppler and Landschützer, 2019; Nevison et al., 2020). Keppler and Landschützer (2019), for example, found increased upwelling and CO_2 outgassing in higher latitudes during positive SAM conditions but opposing effects in other regions. Several data- (Fay et al., 2014; Landschützer et al., 2015; Takahashi et al., 2012) and modeling-based (Le Quéré et al., 2007; Lovenduski et al., 2007, 2008, 2015) studies suggest decadal-scale variability of Southern Ocean CO_2 uptake is within ±0.4 Pg C yr^{-1}, a significant portion of the climatological mean estimate of -0.8 to -1.0 Pg C yr^{-1}.

New observations, however, challenge whether the Southern Ocean is a strong sink. Biogeochemical float data from 2014–2017 estimate a Southern Ocean CO_2 flux of -0.08 Pg C yr^{-1} (Gray et al., 2018), an order of magnitude less than the climatological mean estimates based on ship-based surface ocean CO_2 partial pressure (pCO_2) data products (Landschützer et al., 2016, 2014; Rödenbeck et al., 2015; Takahashi et al., 2009). Even after correcting for a potential bias of 4 µatm to the float-based calculated seawater pCO_2, discrepancies between ship- and float-based CO_2 flux estimates remain (Bushinsky et al., 2019). Whether recent float-based CO_2 flux estimates represent an updated understanding of the climatological mean, float-based seawater pCO_2 requires an even larger bias correction, or 2014–2017 conditions were anomalous, is currently unresolved.

A criticism of ship-based estimates is the scarcity of data in both time and space, especially during winter months. However, surface ocean pCO_2 is measured directly on ships with low uncertainty (±0.5%) (Pierrot et al., 2009), compared to pCO_2 calculated from float pH measurements and estimated total alkalinity that has a higher uncertainty (±2.8%) (Bushinsky et al., 2019; Williams et al., 2017). Unlike ships, floats are able to sample in harsh winter conditions unfit for safe ship operations as well as under ice, increasing the potential for filling observational gaps. Another issue impacting the uncertainty in both float- and ship-based climatological CO_2 flux estimates is the use of observation-derived atmospheric CO_2 products and satellite-based wind and sea level pressure products, which have been shown to add significant uncertainty to CO_2 flux estimates in some regions (Chiodi et al., 2019; Roobaert et al., 2018; Sutton et al., 2017).

Technological advances of Uncrewed Surface Vehicles (USVs) address these observational challenges through remote surveying in harsh conditions with direct measurements of air-sea pCO_2 and wind speed. Here we present results from the first autonomous circumnavigation of Antarctica, a 22,000-km, 196-day mission. A Saildrone Inc. USV with an integrated Autonomous Surface Vehicle CO_2 ($ASVCO_2$™) system was designed specifically to survive the forces of being rolled and submerged by 15-meter breaking waves in the Southern Ocean. We calculate air-sea CO_2 flux from the USV and provide a thorough comparison of potential bias in CO_2 flux calculated with direct measurements relative to recent float-based methods (Bushinsky et al., 2019; Gray et al., 2018) and a ship-based data product (Landschützer et al., 2020) that rely on other satellite- and observational-based data products. We then discuss the potential role of flux uncertainty and interannual variability in determining the Southern Ocean carbon sink.

2 Materials and Methods

2.1 USV and sensors

The Saildrone USV is an ocean-going drone navigable via satellite communications with wind-driven propulsion and primarily solar-powered meteorological and surface ocean physical, chemical, and biological sensors. The Saildrone USV that completed the 2019 Antarctica circumnavigation is similar to the standard vehicles with a 7 m hull and 2.5 m keel described by Meinig et al. (2019) and Zhang et al. (2019) but includes an adapted wing to survive the extreme, high winds and waves of the Southern Ocean (Figure 1). This USV design includes a lower-aspect square rig designed to withstand the force of being rolled and submerged by 15 m breaking waves but limits navigation to sailing primarily downwind. This design has been recently modified to improve maneuverability.

Meteorological sensors are mounted on the square wing, including a Gill WindMaster™ anemometer at 3.8 m height. Through field intercomparisons, Zhang et al. (2019) found RMS differences of ±0.6–1.0 m s^{-1} between wind speed measured on Saildrone USVs with the standard 5 m wing compared to both the Woods Hole Oceanographic Institute's buoy Air-Sea Interaction METeorology System and the R/V *Revelle*. In this study, we use the higher-bound wind speed error of ±1.0 m s^{-1} derived by Zhang et al. (2019) for the estimated error of wind speed measured from the shorter wing at 3.8 m. Even though they determined that bias was inconclusive, to generate conservative estimates we use the mean bias determined from Zhang et al. (2019) intercomparisons of +0.2 m s^{-1}.

The $ASVCO_2$™ system is packaged in a waterproof enclosure mounted in the USV hull. The $ASVCO_2$ is nearly identical to the Moored Autonomous pCO_2 ($MAPCO_2$™) system that has been used for over two decades on dozens of surface buoys and has a lab- and field-validated uncertainty of ±2 μatm or ±0.5% (Sabine et al., 2020; Sutton et al., 2014). These CO_2 systems utilize an equilibrator-based gas collection system and an infrared gas analyzer (LI-820, LI-COR™) calibrated in situ with reference gas traceable to World Meteorological Organization standards, a similar methodology to the underway pCO_2 system deployed on the global network of ships of opportunity (Pierrot et al., 2009). In order to adapt the $MAPCO_2$ for USV deployments, the $ASVCO_2$ includes an equilibrator mounted to the USV hull with a fairing added to maintain consistent water level in the equilibrator when moving at speeds greater than 4 knots (Figure 1).

The $ASVCO_2$ system collects 1-hourly measurements of sea surface and marine boundary layer atmospheric xCO_2 (the mole fraction of CO_2) and sea level atmospheric pressure. Each xCO_2 measurement is paired with sea surface temperature (SST) and salinity (SSS) collected by an RBR Saildrone[3] CTD customized for mounting through the Saildrone USV keel at 0.5 m depth. Seawater and air pCO_2 (at in situ SST) is calculated according to standard operating procedures (Dickson et al., 2007; Weiss, 1974) as described in Sutton et al. (2014). Data from the ASVCO_2 system and wind speed, SST, and SSS are archived at the National Centers for Environmental Information (Sutton et al., 2020).

The USV was deployed from Bluff, New Zealand on 19 January 2019. Sailing downwind, the USV navigated east 22,000 km around Antarctica and was recovered off Bluff on 3 August 2019, 196 days later. The anemometer was damaged near the Drake Passage during an iceberg collision at the end of March.

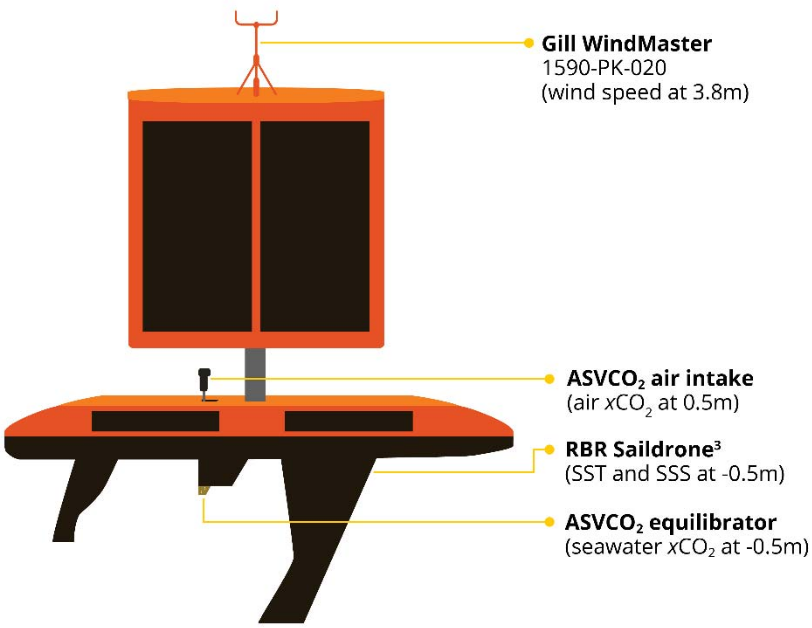

Figure 1. Schematic diagram of the 2019 Southern Ocean Saildrone USV and location of the sensors used in this study. Schematic is not to scale.

2.2 Comparison data sets

Several data sets are used as comparisons for the USV-derived CO_2 fluxes. The first is v2020 of the SOM-FFN neural network product documented in Landschützer et al. (2016), which uses ship-based measurements of seawater pCO_2 to estimate monthly air-sea CO_2 fluxes globally over the period 1982 to 2019 (Landschützer et al., 2020). The second product is the same SOM-FFN neural network, but with the addition of Southern Ocean Carbon and Climate Observations and Modeling project (SOCCOM) float-derived pCO_2 as training datasets (Bushinsky et al., 2019). This product is available as “SOCCOM-only” as well as “SOCCOM+ship” for the years 2014 to 2017. To compare these two data sets with the USV, we subsample each product at the location and month of each USV CO_2 flux measurement and average the CO_2 fluxes over 10-day periods.

The third comparison dataset is air-sea CO_2 fluxes estimated from calculated surface ocean pCO_2 from SOCCOM biogeochemical float data from 2015 to 2019, which is available online as a quality-controlled data snapshot dated 30 August 2020 (Johnson et al., 2020). All float profiles from 2015 to 2019 were separated by year and front locations, and subsequently averaged by month to create monthly pCO_2 and CO_2 flux estimates for each of the three major zones discussed in this manuscript. The Subantarctic Zone is defined as profiles with an oxygen minimum deeper than 1200 m, a salinity maximum deeper than 500 m, and surface waters fresher than 34.6. The Polar Frontal zone is defined as profiles with an oxygen minimum between 900 and 1200 m deep and a deep (>1400 m) salinity maximum. The Antarctic Zone is defined as profiles with an oxygen minimum between 600 and 900 m deep and a salinity maximum deeper than 1000 m. While there are some profiles within the Seasonal Sea Ice Zone which fall within the definitions above, these profiles are not included in the analysis if they occur during a calendar year when that float profiled under ice. In contrast to previous studies, the float profiles have not been extrapolated over time and the monthly averages only represent averages of the instantaneous fluxes at the time of the float surfacing.

We use CO_2 flux provided by the first two comparison data sets (Bushinsky et al., 2019 and Landschützer et al., 2020). CO_2 flux for the third comparison data set (SOCCOM biogeochemical floats from 2015 to 2019) and the USV are calculated using established methodologies summarized in the Supplemental.

3 Results and discussion

3.1 Air-sea observations

During the mission, the USV observed a large range in ΔpCO_2 (seawater – air pCO_2) of 33 to -40 µatm with a slightly negative mean of -4 µatm and a variance of ± 12 µatm (Figure 2). Although periods of negative and positive ΔpCO_2 were observed throughout the deployment, positive ΔpCO_2 indicating outgassing was prevalent during the latter part of the deployment, primarily during late fall and early winter in the Indian Ocean sector of the Antarctic Zone (Figure S1). Observed mean, variation, and range of air xCO_2, sea pCO_2, ΔpCO_2, SST, SSS, and wind speed are given in Table S2.

3.2 CO_2 flux uncertainty analysis

The uncertainty in calculated CO_2 flux can vary widely given the different options of inputs. The gas transfer velocity (k) uncertainty of 20% applies to all CO_2 flux estimates (Wanninkhof, 2014), leaving the choice and availability of wind speed, seawater pCO_2, and air pCO_2 data sets the major sources of variation among different approaches.

Given the scarcity of in situ wind speed observations, the use of satellite-based wind speed in calculating CO_2 flux is common. However, in many regions, these satellite-based products have biases in comparison to available in situ data (Hihara et al., 2015; Kent et al., 2013; Tomita et al., 2015; Wallcraft et al., 2009; Weissman et al., 2012) and can have significant impacts on CO_2 flux estimates (Chiodi et al., 2019; Roobaert et al., 2018; Sutton et al., 2017). Directly-measured wind speed also suffer errors due to flow distortion, platform movement, and wave shadowing, resulting in uncertainties of ±0.1 m s^{-1} on buoys (Cronin et al., 2008; Kubota et al., 2008; Weller, 2015) and up to ±1.0 m s^{-1} on Saildrone USVs (Zhang et al., 2019).

Prior to the USV anemometer being damaged in March 2019, there is no mean difference between USV-measured and Cross-Calibrated Multi-Platform Near Real Time V2.0 (CCMP V2) wind speed (Mears et al., 2019) or ERA-Interim Reanalysis (Dee et al., 2011) wind speed with a variance around wind speed residuals of ±1.8 m s^{-1} and ±2.0 m s^{-1}, respectively (Figure S2). NCEP-DOE AMIP-II Reanalysis 2 (NCEP-2) (Kanamitsu et al., 2002) and ERA5 (Hersbach et al., 2020) wind speeds have lower wind speed by 1.0 and 0.1 m s^{-1}, respectively, than measured on the USV with a variance around the mean bias of ±3.9 and ±1.4 m s^{-1}, respectively. In Table S1 these biases are reported relative to the "true" wind speed by correcting for the USV wind speed bias of +0.2 m s^{-1} (Zhang et al., 2019). Importantly, the biases in satellite-based wind speed products relative to the USV-measured wind speed are not randomly distributed. Satellite and USV wind speeds tend to agree most closely at wind speeds of 10 m s^{-1}, but diverge at lower and higher wind speeds (Figure S2c). These results are consistent with biases reported in other intercomparisons mentioned previously and summarized by Cronin et al. (2019).

Uncertainties associated with ship-, USV-, and float-based sources of pCO_2 are ±0.5%, ±0.5%, and ±2.8%, respectively (Table S1.) Common data sources of atmospheric baseline xCO_2 are the NOAA Greenhouse Gas Marine Boundary Layer (MBL) Reference CO_2 product (Dlugokencky et al., 2019) or observations from nearby atmospheric observatories, like at Cape Grim. Monthly mean xCO_2 from these two sources and the USV tend to agree within 0.2 ppm; however, shorter-term variability indicating terrestrial biosphere influence is prevalent within the hourly USV observations (Figure S3) and the hourly in situ Cape Grim observations (data not shown). Converting these sources of xCO_2 to pCO_2 requires atmospheric pressure at sea level, which if using satellite-based products such as NCEP 2, ERA-Interim, or ERA5 introduces another possible source of error (Table S1).

Various sampling frequencies of these data sources can also introduce error into the CO_2 flux calculation. Monthly CO_2 flux calculated from subsampling the hourly USV ΔpCO_2 data set at 6-hourly intervals, which is the common temporal frequency of satellite-based products, results in nearly identical values to monthly flux calculated from the hourly observations (Figure S4). However, subsampling the hourly data set at all possible 10-day sampling frequencies, the timescale for float observations, results in an integrated bias in CO_2 flux of +0.05 g C m^{-2} mo^{-1} or +23% (less uptake/more outgassing) over the 7-month comparison period with large variation around the monthly means due to the high temporal variability of the data set at a scale of less than 10 days.

Propagated bias of USV-derived CO_2 flux is -4% (less outgassing/more uptake) driven by the potential bias in USV-measured wind speed (Table 1). In this case, USV, CCMP V2, and ERA-Interim wind speed bias are equivalent and have the same impact on calculated CO_2 flux. Replacing directly-measured air pCO_2 with pCO_2 calculated from MBL or Cape Grim values and NCEP 2, ERA-Interim, or ERA5 sea level pressure does not significantly impact flux bias. Taking into consideration the potential bias of subsampling at 10-day intervals combined with the ERA-Interim wind speed bias results in an overall positive bias of +20% (more outgassing/less uptake) in calculated CO_2 flux primarily due to the bias in subsampling the 2019 USV data set at 10-day intervals. Monteiro et al. (2015) found that a 10-day sampling period in spring-summer in the Subantarctic Zone resulted in a 10-25% increase in uncertainty in CO_2 flux relative to hourly sampling due to mixed layer responses to storm events, which may explain a similar magnitude sampling bias observed with the USV results.

Table 1. Estimated bias for different approaches of calculating CO_2 flux by applying mean bias from Table S1 to conditions observed during the 2019 USV deployment. Resulting biases are additive based on mean biases reported in Table S1. A negative bias suggests less outgassing/more uptake; positive suggests more outgassing/less uptake. The USV CO_2 flux bias results from the estimated USV wind speed bias of +0.2 m s^{-1} (Zhang et al., 2019).

Seawater pCO_2 data source	Air pCO_2 data source	Wind speed data source	Estimated CO_2 flux bias
USV	USV	USV	-4%
Ship or USV	Ship, USV, MBL, or Gape Grim	CCMP-NRT or ERA-Interim	-4%
Float-derived	MBL or Cape Grim	ERA-Interim	+20%

3.3 CO_2 flux comparisons

Due to the loss of the wind speed sensor during the USV deployment, USV CO_2 flux presented in this section is calculated using CCMP V2 wind speed. During the 2019 circumnavigation, the USV observed periods of strong outgassing as high as 10.5 g C m^{-2} mo^{-1} in June and July in the Antarctic Zone, which was one of the zones where SOCCOM float-based data from 2014–2017 showed stronger outgassing than the SOM-FFN ship-based climatology (Figure 3a; Bushinsky et al., 2019; Gray et al., 2018). There were also periods of intense short-scale CO_2 uptake during February through April, some of which were associated with phytoplankton blooms (data not shown). The periods of strong outgassing observed by the USV in June and July overlap with the Bushinsky et al. (2019) 2014–2017 SOCCOM-only SOM-FFN estimates of CO_2 outgassing (Figure 3a). However, the USV observations show these outgassing events occur over time periods from hours to two days in length, and these short-lived outgassing events do not lead to outgassing as strong as the SOCCOM-only SOM-FFN estimates when averaged at the 10-day scale. Mean USV CO_2 flux in June and July results in a weak net outgassing of 0.7 g C m^{-2} mo^{-1}, more similar to the Landschützer et al. (2020) ship-based data product and the Bushinsky et al. (2019) combined SOCCOM-ship SOM-FFN product than the SOCCOM-only SOM-FFN product.

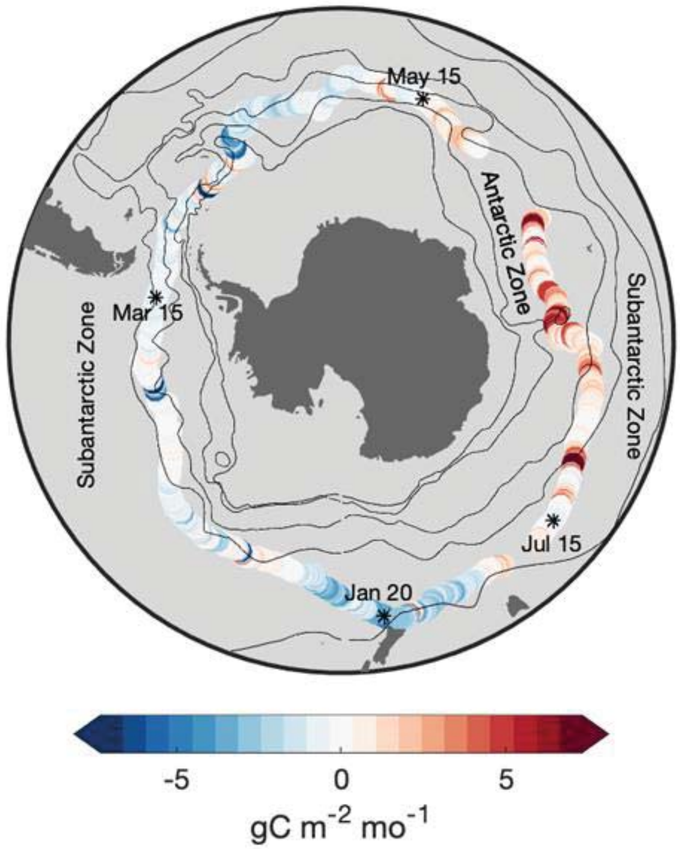

Figure 2. CO_2 flux calculated from USV-measured ΔpCO_2, SST, and SSS and CCMP-NRT wind speed. Dates and * show the location of the USV with time. Black lines indicate climatological locations of the major fronts from Orsi et al. (1995) as in Figure S1.

Focusing only on 2019 observations, USV-measured and float-estimated surface seawater pCO_2 are consistent within standard deviations of monthly means within the Subantarctic Zone and the Antarctic Zone, the two major zones sampled by the 2019 Saildrone USV (Figure S5). Within the Antarctic Zone where Gray et al. (2018) found the largest winter-time discrepancy between float- and ship-based data, we find a mean difference of 0.5 ± 2.6 g C m^{-2} mo^{-1} (or no significant difference) between USV and float-derived CO_2 flux in March through July 2019 (Figure 3b). To test the possible effect of variable float locations on the estimates of CO_2 flux in the Antarctic Zone, the Landschützer v2020 SOM-FFN ship-based climatology was subsampled at the times and locations of each float observation. Float-based fluxes are on average 1.5 g C m^{-2} mo^{-1} greater than the ship-based climatology in this zone for 2015–2019 with significant interannual variability (2015: +3.9, 2016: +2.1, 2017: +0.6, 2018: +0.8, and 2019: -0.1 g C m^{-2} mo^{-1}).

Figure 3b illustrates this significant interannual variability in float-derived CO_2 flux in the Antarctic Zone from 2015–2019. Net CO_2 uptake observed by the USV and floats in 2019 contrasts with the strong outgassing during winter of 2015 and 2016. This interannual variability may be influenced by SAM with increased westerly wind strength during the more positive phases of SAM increasing upwelling of relatively CO_2-rich waters. The greatest outgassing is observed in the Antarctic Zone during strong positive phases of SAM in 2015 and 2016 (Figures 3b and S6). The USV data were collected during a decline in the SAM index and are similar to the float-based net flux estimates for 2019 (Figure 3b).

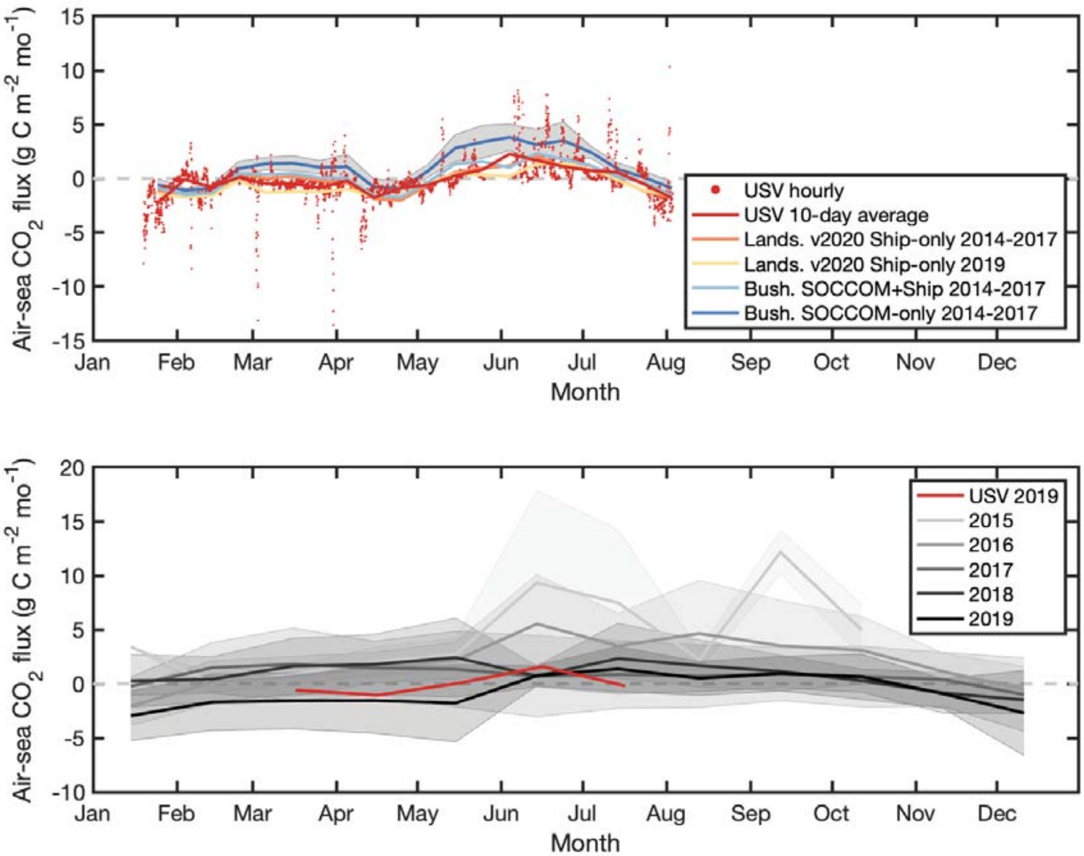

Figure 3. a) Time series of monthly CO_2 flux calculated using all USV observations at hourly (red dots) and 10-day averaged (red line) time steps; from Landschützer et al. (2020) SOM-FFN ship-based climatology (orange) and 2019 (yellow) subsampled at the Saildrone locations and times and averaged over 10 days; and from Bushinsky et al. (2019) using the same methods of the SOM-FFN v2020 ship-based climatology for the years 2014–2017 but incorporating seawater pCO_2 estimated from both ships and SOCCOM biogeochemical-float observations (light blue), and using only SOCCOM biogeochemical float observations (dark blue) for the years 2014–2017. The shaded area represents the interannual variability in the SOCCOM-only product over 2014–2017. b) Antarctic Zone monthly-averaged USV fluxes (red) plotted with monthly mean SOCCOM float-based CO_2 flux from 2015–2019 in that zone (gray). The shaded area is 1 σ of monthly mean SOCCOM CO_2 flux.

Analysis of the Saildrone USV observations reveal several potential sources of bias and error in USV-, ship-, and float-based CO_2 flux (Tables S1 and 1). Given the significant fine-scale temporal and spatial variability observed during 2019, the 10-day sampling routine of floats may introduce a bias (more outgassing/less uptake in this case), which could account for some of the difference between float- and ship-based CO_2 flux reported previously (Bushinsky et al., 2019; Gray et al., 2018). It is also critical to better constrain how shifts in SAM conditions play a role in Southern Ocean CO_2 flux. The larger differences between the ship-based climatology and float-based flux during prolonged positive SAM conditions in 2015–2016 suggests an influence of measurement bias during those years or the possibility that the ship-based climatology does not constrain increased upwelling of CO_2-rich water in higher latitudes. Sustained observations are needed to better constrain interannual variability like the anomalous strong winter outgassing observed by floats in 2015–2016 relative to 2017–2019. Better coverage of ships, USVs, and floats are needed to resolve these uncertainties in measurements and variability in the Southern Ocean.

4 Conclusions

Climate change is predicted to reduce ocean CO_2 uptake under climate model scenarios that show intensification of winds and acceleration of the overturning circulation in the Southern Ocean (Le Quéré et al., 2007). Over the next century models also predict reductions in sea-ice cover and surface ocean warming, freshening, and stratification, which are all expected to impact the carbon sink. How these processes impact the overall balance of CO_2 outgassing and uptake in the Southern Ocean is uncertain. Better representation of these processes in models is necessary to predict the Southern Ocean's role in a future climate.

Our results indicate that the strong wintertime outgassing observed by floats in 2015 and 2016 was not prevalent in 2019. The change may be linked to a decline in the SAM index in the later years leading to a reduction in upwelling of CO_2 rich waters to the surface. More sustained observations are needed to constrain interannual variability and the impact on both Southern Ocean and global ocean CO_2 uptake estimates. The first circumnavigation of the Southern Ocean by a USV described here has shown the capability to collect high quality data that can be used to constrain multi-platform measurement uncertainties and interrogate how variability from the scale of hours to years may impact CO_2 flux estimates.

A multi-platform observing network consisting of USVs directly surveying air-sea interactions, floats measuring full water column biogeochemistry even under ice, and the ship-based measurements for ground-truthing autonomous sensors would, in combination, best track changes in ocean carbon uptake and better constrain variability. USVs fill a unique niche with the ability to survey regions for extended periods where ships do not routinely operate, opening up new opportunities for filling persistent gaps in the ocean observing system with high-quality pCO_2 and meteorological observations.

Acknowledgments

We acknowledge the generous support of Li Ka Shing Foundation for funding the Saildrone USV platform circumnavigation of Antarctica and Saildrone Inc. for coordination and operation of the circumnavigation and delivering real-time data. $ASVCO_2$™ development and field evaluations were supported by the Office of Oceanic and Atmospheric Research of the NOAA, U.S. Department of Commerce, including resources from the Global Ocean Monitoring and Observation program and the Pacific Marine Environmental Laboratory (PMEL). $ASVCO_2$™ development was led by PMEL scientists and engineers including Noah Lawrence-Slavas, Randy Bott, and Stacy Maenner. The USV data used here are available at https://doi.org/10.25921/6zja-cg56 (Sutton et al., 2020). The biogeochemical Argo float data were collected and made freely available by the Southern Ocean Carbon and Climate Observations and Modeling (SOCCOM) Project funded by the National Science Foundation, Division of Polar Programs (NSF PLR -

1425989), supplemented by NASA, and by the International Argo Program and the NOAA programs that contribute to it. Data are available through Sutton et al. 2020. BT was supported by the Australian Antarctic Program Partnership and the Australian Integrated Marine Observing System. This is PMEL contribution 5181.

References

Bushinsky, S. M., Landschützer, P., Rödenbeck, C., Gray, A. R., Baker, D., Mazloff, M. R., et al. (2019). Reassessing Southern Ocean air-sea CO_2 flux estimates with the addition of biogeochemical float observations. *Global Biogeochemical Cycles, 33*(11), 1370–1388. https://doi.org/10.1029/2019GB006176

Chiodi, A. M., Dunne, J. P., & Harrison, D. E. (2019). Estimating air-sea carbon flux uncertainty over the tropical Pacific: Importance of winds and wind analysis uncertainty. *Global Biogeochemical Cycles, 33*, 370–390. https://doi.org/10.1029/2018GB006047

Cronin, M. F., Gentemann, C. L., Edson, J., Ueki, I., Bourassa, M., Brown, S., et al. (2019). Air-sea fluxes with a focus on heat and momentum. *Frontiers in Marine Science, 6*, 430. https://doi.org/10.3389/fmars.2019.00430

Cronin, M. F., Meinig, C., Sabine, C. L., Ichikawa, H., & Tomita, H. (2008). Surface mooring network in the Kuroshio Extension. *IEEE Systems Special Issue on GEOSS, 2*(3), 424–430.

Dee, D. P., Uppala, S. M., Simmons, A. J., Berrisford, P., Poli, P., Kobayashi, S., et al. (2011). The ERA-Interim reanalysis: configuration and performance of the data assimilation system. *Quarterly Journal of the Royal Meteorological Society, 137*(656), 553–597. https://doi.org/10.1002/qj.828

Dickson, A. G., Sabine, C. L., & Christian, J. R. (Eds.). (2007). *Guide to Best Practices for Ocean CO_2 Measurements*: North Pacific Marine Science Organization.

Dlugokencky, E. G., Thoning, K. W., Lang, P. M., & Tans, P. P. (2019). NOAA Greenhouse Gas Reference from Atmospheric Carbon Dioxide Dry Air Mole Fractions from the NOAA ESRL Carbon Cycle Cooperative Global Air Sampling Network. Data Path: ftp://aftp.cmdl.noaa.gov/data/trace_gases/co2/flask/surface/ [Accessed 1 August 2019]

Fay, A. R., McKinley, G. A., & Lovenduski, N. S. (2014). Southern Ocean carbon trends: Sensitivity to methods. *Geophysical Research Letters, 41*(19), 6833–6840. https://doi.org/10.1002/2014GL061324

Frölicher, T. L., Sarmiento, J. L., Paynter, D. J., Dunne, J. P., Krasting, J. P., & Winton, M. (2014). Dominance of the Southern Ocean in anthropogenic carbon and heat uptake in CMIP5 models. *Journal of Climate, 28*(2), 862–886. https://doi.org/10.1175/JCLI-D-14-00117.1

Gray, A. R., Johnson, K. S., Bushinsky, S. M., Riser, S. C., Russell, J. L., Talley, L. D., et al. (2018). Autonomous biogeochemical floats detect significant carbon dioxide outgassing in the high-latitude Southern Ocean. *Geophysical Research Letters, 45*(17), 9049–9057. https://doi.org/10.1029/2018GL078013

Hersbach, H., Bell, B., Berrisford, P., Hirahara, S., Horányi, A., Muñoz-Sabater, J., et al. (2020). The ERA5 global reanalysis. 146(730), 1999-2049.

Hihara, T., Kubota, M., & Okuro, A. (2015). Evaluation of sea surface temperature and wind speed observed by GCOM-W1/AMSR2 using in situ data and global products. *Remote Sensing of Environment, 164*, 170–178. https://doi.org/10.1016/j.rse.2015.04.005

Iudicone, D., Rodgers, K. B., Stendardo, I., Aumont, O., Madec, G., Bopp, L., et al. (2011). Water masses as a unifying framework for understanding the Southern Ocean carbon cycle. *Biogeosciences, 8*(5), 1031–1052. https://doi.org/10.5194/bg-8-1031-2011

Johnson, K. S., Riser, S. C., Boss, E. S., Talley, L. D., Sarmiento, J. L., Swift, D. D., et al. (2020). SOCCOM float data - Snapshot 2020-08-30. In Southern Ocean Carbon and Climate Observations and Modeling (SOCCOM) Float Data Archive. UC San Diego Library Digital Collections. https://doi.org/10.6075/J0BK19W5

Kanamitsu, M., Ebisuzaki, W., Woollen, J., Yang, S.-K., Hnilo, J. J., Fiorino, M., & Potter, G. L. (2002). NCEP–DOE AMIP-II Reanalysis (R-2). *Bulletin of the American Meteorological Society, 83*(11), 1631–1644. https://doi.org/10.1175/BAMS-83-11-1631

Kent, E. C., Fangohr, S., & Berry, D. I. (2013). A comparative assessment of monthly mean wind speed products over the global ocean. *International Journal of Climatology, 33*(11), 2520–2541. https://doi.org/10.1002/joc.3606

Keppler, L., & Landschützer, P. (2019). Regional wind variability modulates the Southern Ocean carbon sink. *Scientific Reports, 9*(1), 7384. https://doi.org/10.1038/s41598-019-43826-y

Khatiwala, S., Primeau, F., & Hall, T. (2009). Reconstruction of the history of anthropogenic CO_2 concentrations in the ocean. *Nature, 462*(7271), 346–349. https://doi.org/10.1038/nature08526

Kubota, M., Iwabe, N., Cronin, M. F., & Tomita, H. (2008). Surface heat fluxes from the NCEP/NCAR and NCEP/DOE reanalyses at the KEO buoy site. *Journal of Geophysical Research Oceans, 113*, C02009.

Landschützer, P., Gruber, N., & Bakker, D. C. E. (2016). Decadal variations and trends of the global ocean carbon sink. *Global Biogeochemical Cycles, 30*(10), 1396–1417. https://doi.org/10.1002/2015GB005359

Landschützer, P., Gruber, N., & Bakker, D. C. E. (2020). An observation-based global monthly gridded sea surface pCO_2 product from 1982 onward and its monthly climatology (NCEI Accession 0160558). Version 5.5. NOAA National Centers for Environmental Information. Dataset. https://doi.org/10.7289/V5Z899N6 [Accessed 2020-07-10]

Landschützer, P., Gruber, N., Bakker, D. C. E., & Schuster, U. (2014). Recent variability of the global ocean carbon sink. *Global Biogeochemical Cycles, 28*, 927–949. https://doi.org/10.1002/2014GB004853

Landschützer, P., Gruber, N., Haumann, F. A., Rödenbeck, C., Bakker, D. C. E., van Heuven, S., et al. (2015). The reinvigoration of the Southern Ocean carbon sink. *Science, 349*(6253), 1221–1224. https://doi.org/10.1126/science.aab2620

Large, W. G., & Pond, S. (1981). Open ocean momentum flux measurements in moderate to strong winds. *Journal of Physical Oceanography, 11*(3), 324–336. https://doi.org/10.1175/1520-0485(1981)011<0324:OOMFMI>2.0.CO;2

Le Quéré, C., Rödenbeck, C., Buitenhuis, E. T., Conway, T. J., Langenfelds, R., Gomez, A., et al. (2007). Saturation of the Southern Ocean CO_2 sink due to recent climate change. *Science, 316*(5832), 1735–1738. https://doi.org/10.1126/science.1136188

Lovenduski, N. S., Fay, A. R., & McKinley, G. A. (2015). Observing multidecadal trends in Southern Ocean CO_2 uptake: What can we learn from an ocean model? *Global Biogeochemical Cycles, 29*(4), 416–426. https://doi.org/10.1002/2014GB004933

Lovenduski, N. S., Gruber, N., & Doney, S. C. (2008). Toward a mechanistic understanding of the decadal trends in the Southern Ocean carbon sink. *Global Biogeochemical Cycles, 22*(3), GB3016. https://doi.org/10.1029/2007GB003139

Lovenduski, N. S., Gruber, N., Doney, S. C., & Lima, I. D. (2007). Enhanced CO_2 outgassing in the Southern Ocean from a positive phase of the Southern Annular Mode. *Global Biogeochemical Cycles, 21*(2), GB2026. https://doi.org/10.1029/2006GB002900

Marshall, G. J. (2003). Trends in the Southern Annular Mode from observations and reanalyses. *Journal of Climate, 16*(24), 4134–4143. https://doi.org/10.1175/1520-0442%282003%29016%3C4134%3ATITSAM%3E2.0.CO%3B2

Mears, C. A., Scott, J., Wentz, F. J., Ricciardulli, L., Leidner, S. M., Hoffman, R., & Atlas, R. (2019). A near-real-time version of the Cross-Calibrated Multiplatform (CCMP) ocean surface wind velocity data set. *Journal of Geophysical Research Oceans, 124*(10), 6997–7010. https://doi.org/10.1029/2019JC015367

Meinig, C., Burger, E. F., Cohen, N., Cokelet, E. D., Cronin, M. F., Cross, J. N., et al. (2019). Public–private partnerships to advance regional ocean-observing capabilities: A Saildrone and NOAA-PMEL case study and future considerations to expand to global scale observing. *Frontiers in Marine Science, 6,* 448. https://doi.org/10.3389/fmars.2019.00448

Monteiro, P. M. S., Gregor, L., Lévy, M., Maenner, S., Sabine, C. L., & Swart, S. (2015). Intraseasonal variability linked to sampling alias in air-sea CO_2 fluxes in the Southern Ocean. *Geophysical Research Letters, 42*(20), 8507–8514. https://doi.org/10.1002/2015GL066009

Nevison, C. D., Munro, D. R., Lovenduski, N. S., Keeling, R. F., Manizza, M., Morgan, E. J., & Rödenbeck, C. (2020). Southern Annular Mode influence on wintertime ventilation of the Southern Ocean detected in atmospheric O2 and CO2 measurements. *Geophysical Research Letters, 47*, e2019GL085667. https://doi.org/10.1029/2019GL085667

Orsi, A. H., Whitworth, T., & Nowlin, W. D. (1995). On the meridional extent and fronts of the Antarctic Circumpolar Current. *Deep Sea Research Part I: Oceanographic Research Papers, 42*(5), 641–673. https://doi.org/10.1016/0967-0637(95)00021-W

Pierrot, D., Neill, C., Sullivan, K., Castle, R., Wanninkhof, R., Lüger, H., et al. (2009). Recommendations for autonomous underway pCO_2 measuring systems and data-reduction routines. *Deep Sea Research Part II: Topical Studies in Oceanography, 56*(8–10), 512–522. https://doi.org/10.1016/j.dsr2.2008.12.005

Rödenbeck, C., Bakker, D. C. E., Gruber, N., Iida, Y., Jacobson, A. R., Jones, S., et al. (2015). Data-based estimates of the ocean carbon sink variability – first results of the Surface Ocean pCO2 Mapping intercomparison (SOCOM). *Biogeosciences*, 12(23), 7251-7278.

Roobaert, A., Laruelle, G. G., Landschützer, P., & Regnier, P. (2018). Uncertainty in the global oceanic CO_2 uptake induced by wind forcing: quantification and spatial analysis. *Biogeosciences, 15*(6), 1701–1720. https://doi.org/10.5194/bg-15-1701-2018

Sabine, C., Sutton, A., McCabe, K., Lawrence-Slavas, N., Alin, S., Feely, R., et al. (2020). Evaluation of a new carbon dioxide system for autonomous surface vehicles. *Journal of Atmospheric and Oceanic Technology, 37*(8), 1305–1317. https://doi.org/10.1175/JTECH-D-20-0010.1

Sutton, A. J.; Battisti, R., Maenner Jones, S., Musielewicz, S., Bott, R., Osborne, J. (2020). Surface underway measurements of partial pressure of carbon dioxide (pCO_2), sea surface temperature, sea surface salinity and other parameters from Autonomous Surface Vehicle ASV_Saildrone1020 (EXPOCODE 32DB20190119) in the South Atlantic Ocean, South Pacific Ocean, Indian Ocean and Southern Ocean from 2019-01-19 to 2019-08-03 (NCEI Accession 0221912). NOAA National Centers for Environmental Information. doi: https://doi.org/10.25921/6zja-cg56.

Sutton, A. J., Sabine, C. L., Maenner-Jones, S., Lawrence-Slavas, N., Meinig, C., Feely, R. A., et al. (2014). A high-frequency atmospheric and seawater pCO_2 data set from 14 open-ocean sites using a moored autonomous system. *Earth System Science Data, 6*(2), 353–366. https://doi.org/10.5194/essd-6-353-2014

Sutton, A. J., Wanninkhof, R., Sabine, C. L., Feely, R. A., Cronin, M. F., & Weller, R. A. (2017). Variability and trends in surface seawater pCO_2 and CO_2 flux in the Pacific Ocean. *Geophysical Research Letters, 44*(11), 5627–5636. https://doi.org/10.1002/2017GL073814

Takahashi, T., Sutherland, S. C., Wanninkhof, R., Sweeney, C., Feely, R. A., Chipman, D. W., et al. (2009). Climatological mean and decadal change in surface ocean pCO_2, and net sea-air CO_2 flux over the global oceans. *Deep Sea Research Part II: Topical Studies in Oceanography, 56*(8-10), 554–577. https://doi.org/10.1016/j.dsr2.2008.12.009

Takahashi, T., Sweeney, C., Hales, B., Chipman, D. W., Newberger, T., Goddard, J. G., et al. (2012). The changing carbon cycle in the Southern Ocean. *Oceanography, 25*(3), 26–37.

Tomita, H., Kawai, Y., Cronin, M. F., Hihara, T., & Kubota, M. (2015). Validation of AMSR2 sea surface wind and temperature over the Kuroshio Extension region. *SOLA, 11*, 43–47.

Wallcraft, A. J., Kara, A. B., Barron, C. N., Metzger, E. J., Pauley, R. L., & Bourassa, M. A. (2009). Comparisons of monthly mean 10 m wind speeds from satellites and NWP products over the global ocean. *Journal of Geophysical Research: Atmospheres, 114*(D16), D16109. https://doi.org/10.1029/2008JD011696

Wanninkhof, R. (2014). Relationship between wind speed and gas exchange over the ocean revisited. *Limnology and Oceanography: Methods, 12*(6), 351–362. https://doi.org/10.4319/lom.2014.12.351

Watson, A. J., Schuster, U., Shutler, J. D., Holding, T., Ashton, I. G. C., Landschützer, P., et al. (2020). Revised estimates of ocean-atmosphere CO2 flux are consistent with ocean carbon inventory. *Nature Communications*, 11(1), 4422. https://doi.org/10.1038/s41467-020-18203-3

Weiss, R. F. (1974). Carbon dioxide in water and seawater: the solubility of a non-ideal gas. *Marine Chemistry, 2*(3), 203–215. https://doi.org/10.1016/0304-4203(74)90015-2

Weiss, R. F., Jahnke, R. A., & Keeling, C. D. (1982). Seasonal effects of temperature and salinity on the partial pressure of CO_2 in seawater. *Nature, 300*(5892), 511–513. https://doi.org/10.1038/300511a0

Weissman, D. E., Stiles, B. W., Hristova-Veleva, S. M., Long, D. G., Smith, D. K., Hilburn, K. A., & Jones, W. L. (2012). Challenges to satellite sensors of ocean winds: Addressing precipitation effects. *Journal of Atmospheric and Oceanic Technology, 29*(3), 356–374. http://doi.org/10.1175/JTECH-D-11-00054.1

Weller, R. A. (2015). Variability and trends in surface meteorology and air–sea fluxes at a site off northern Chile. *Journal of Climate, 28*(8), 3004-3023. https://doi.org/10.1175/JCLI-D-14-00591.1

Williams, N. L., Juranek, L. W., Feely, R. A., Johnson, K. S., Sarmiento, J. L., Talley, L. D., et al. (2017). Calculating surface ocean pCO_2 from biogeochemical Argo floats equipped with pH: An uncertainty analysis. *Global Biogeochemical Cycles, 31*(3), 591–604. https://doi.org/10.1002/2016GB005541

Zhang, D., Cronin, M. F., Meinig, C., Farrar, J. T., Jenkins, R., Peacock, D., et al. (2019). Comparing air-sea flux measurements from a new unmanned surface vehicle and proven platforms during the SPURS-2 field campaign. *Oceanography, 32*(2), 122–133. https://doi.org/10.5670/oceanog.2019.220

Geophysical Research Letters

Supporting Information for

Constraining Southern Ocean CO_2 Flux Uncertainty Using Uncrewed Surface Vehicle Observations

A. J. Sutton[1], N. L. Williams[2], and B. Tilbrook[3,4]

[1]Pacific Marine Environmental Laboratory, National Oceanic and Atmospheric Administration, Seattle, Washington, USA.

[2]University of South Florida, St. Petersburg, Florida, USA.

[3]Oceans and Atmosphere, Commonwealth Scientific and Industrial Research Organisation, Hobart, Tasmania, Australia.

[4]Australian Antarctic Program Partnership, University of Tasmania, Hobart, Australia.

Contents of this file

Introduction

Additional figures and tables of 2019 Southern Ocean Saildrone USV observations and intercomparisons as well as a summary of CO_2 flux calculations are included here as supporting information.

CO_2 flux calculations

CO_2 flux is calculated using:

$$CO_2 \text{ flux} = k \times K_o \times \Delta pCO_2$$

where k is the gas transfer velocity as a function of wind speed (Wanninkhof, 2014), K_o is the solubility coefficient for CO_2 as a function of SST and SSS (Weiss, 1974; Weiss et al., 1982), and ΔpCO_2 is seawater pCO_2 – air pCO_2.

The ASVCO₂ provides directly-measured seawater and air pCO_2. For the floats, seawater pCO_2 is calculated using measured pH and estimated total alkalinity as described by Williams et al. (2017) and atmospheric pCO_2 is calculated from air xCO2 observations from the NOAA Greenhouse Gas Marine Boundary Layer Reference product (Dlugokencky et al., 2019) converted to pCO_2 using NCEP 2 sea level atmospheric pressure. As noted in the main text, the float fluxes were not extrapolated over time as was done by Gray et al. (2018). This means that the monthly averages presented here are averages of the instantaneous flux at the time of the float surfacing.

Gradients in seawater pCO_2 are assumed insignificant between the Saildrone measurements depth at about 0.5 m and the float measurements depth at 5–7 m in the well-mixed surface waters of the Southern Ocean. These measurements are also well below the surface boundary layer where skin temperature effects could impact the flux comparison between the different measurement approaches (Watson et al., 2020).

Several sources of wind speed have been used in previous studies to calculate CO_2 flux: Cross-Calibrated Multi-Platform Near Real Time V2.0 (CCMP V2) (Mears et al., 2019), NCEP-DOE AMIP-II Reanalysis 2 (NCEP 2) (Kanamitsu et al., 2002), ERA-Interim Reanalysis (Dee et al., 2011), and ERA5 (Hersbach et al., 2020). All wind speed data assessed here are 6-hourly except for ERA5 and USV-measured wind speed, which are hourly resolution. All satellite-based winds used here are at 10 m, with USV wind speed measured at 3.8 m corrected to a height of 10 m using parameterizations of Large and Pond (1981) as described in Sutton et al. (2017).

CCMP V2 wind speed is used to calculate both USV and 2015–2019 SOCCOM biogeochemical float fluxes. For the other two comparison data sets, Landschützer et al. (2020) uses ERA5 wind speed with k scaled for ERA5 wind data, and Bushinsky et al. (2019) uses ERA-Interim using k of Wanninkhof (2014), which is scaled for CCMP wind data.

Given the USV provides hourly in situ air-sea pCO_2 and wind speed observations, the 2019 USV data set is used to estimate potential bias and error in satellite-based wind speed and sea level pressure, different sources of air xCO_2, and the effect of different sampling periods. In Table S1, bias is the mean difference between the USV measurements and these other sources. Error is one standard deviation (σ) of the differences.

The effect of the 10-day sampling period used by biogeochemical floats on monthly flux is estimated by subsampling hourly USV air and seawater pCO_2, SST, and SSS every 10 days at noon (UTC) and linearly interpolating the values in between. These values are then combined with high-frequency wind speed to estimate CO_2 flux. To obtain as many realizations of the mean as possible, this is repeated ten times by shifting the starting time by a day. Resulting bias is the mean difference between the monthly USV flux and monthly mean flux from all realizations of the 10-day subsampling, averaged for each month from January through July.

We also use direct measurements of air-sea pCO_2 and wind speed from the USV, which are rare in the Southern Ocean, as the baseline for interrogating how potential bias in other products and interpolated observations impact calculated CO_2 flux. We estimate this by applying the mean bias in Table S1 directly to the USV wind speed, sea level pressure, seawater pCO_2, and, in the case of sampling frequency, calculated CO_2 flux in the 7-month USV data set. For example, in the case of USV-derived CO_2 flux (first entry in Table 1), the wind speed bias of +0.2 m s^{-1} is applied to the data set, then CO_2 flux is re-calculated. The resulting mean difference between the original USV CO_2

flux and flux with biases applied is reported for each approach in Table 1. This technique of using the 2019 Southern Ocean USV data to estimate calculated CO_2 flux bias is specific to the conditions observed during this mission and may not apply to the bias in these approaches in other applications.

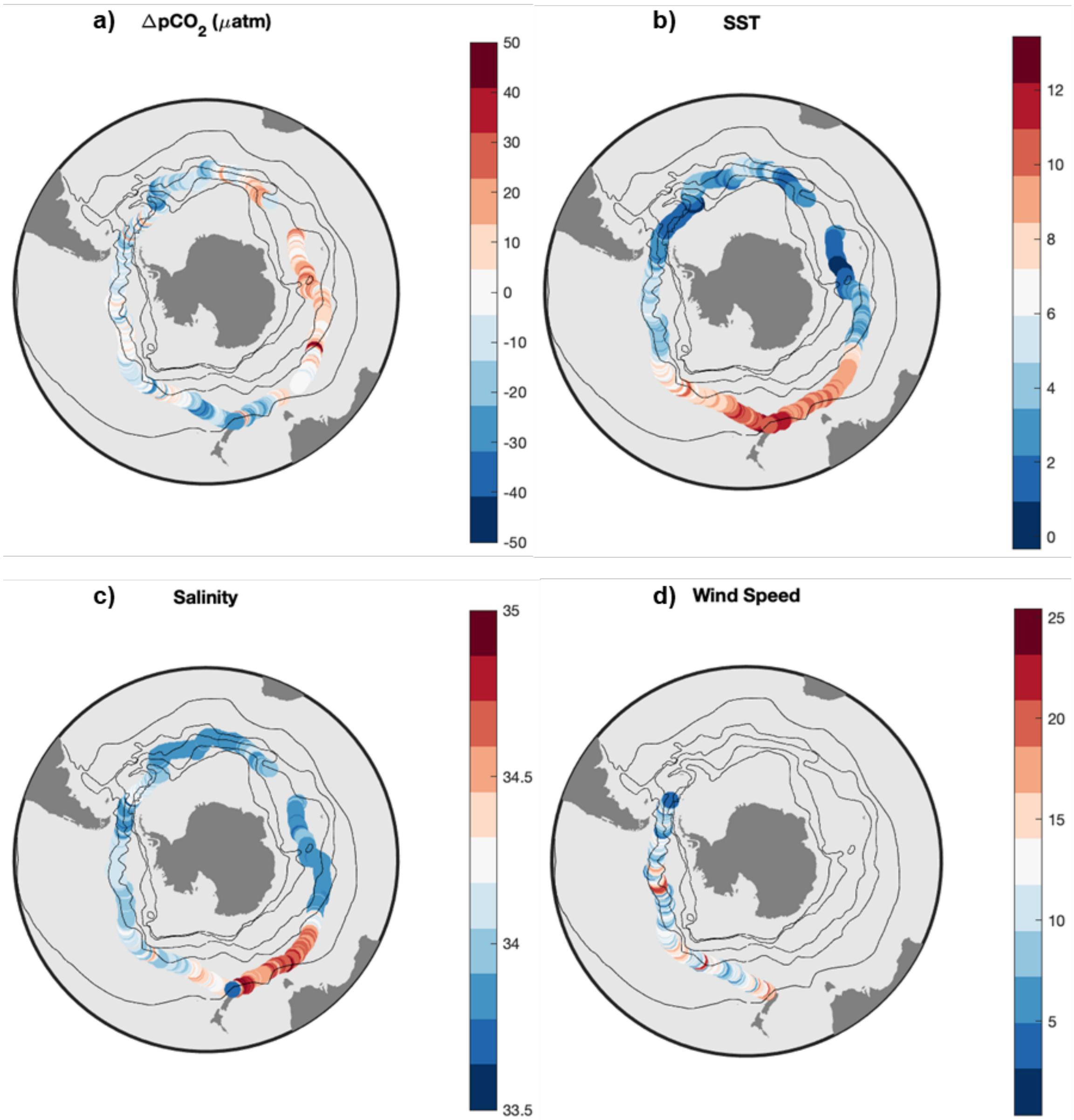

Figure S1. Saildrone USV-measured a) ΔpCO_2 (µatm), b) SST (^oC), c) SSS, and d) wind speed (m s^{-1}) during the mission along with black lines indicating climatological locations of the major fronts from Orsi et al. (1995). Zones moving from Antarctica north are: Seasonal Ice Zone, Antarctic-Southern Zone, Polar Frontal Zone, Subantarctic Zone, and Subtropical Zone.

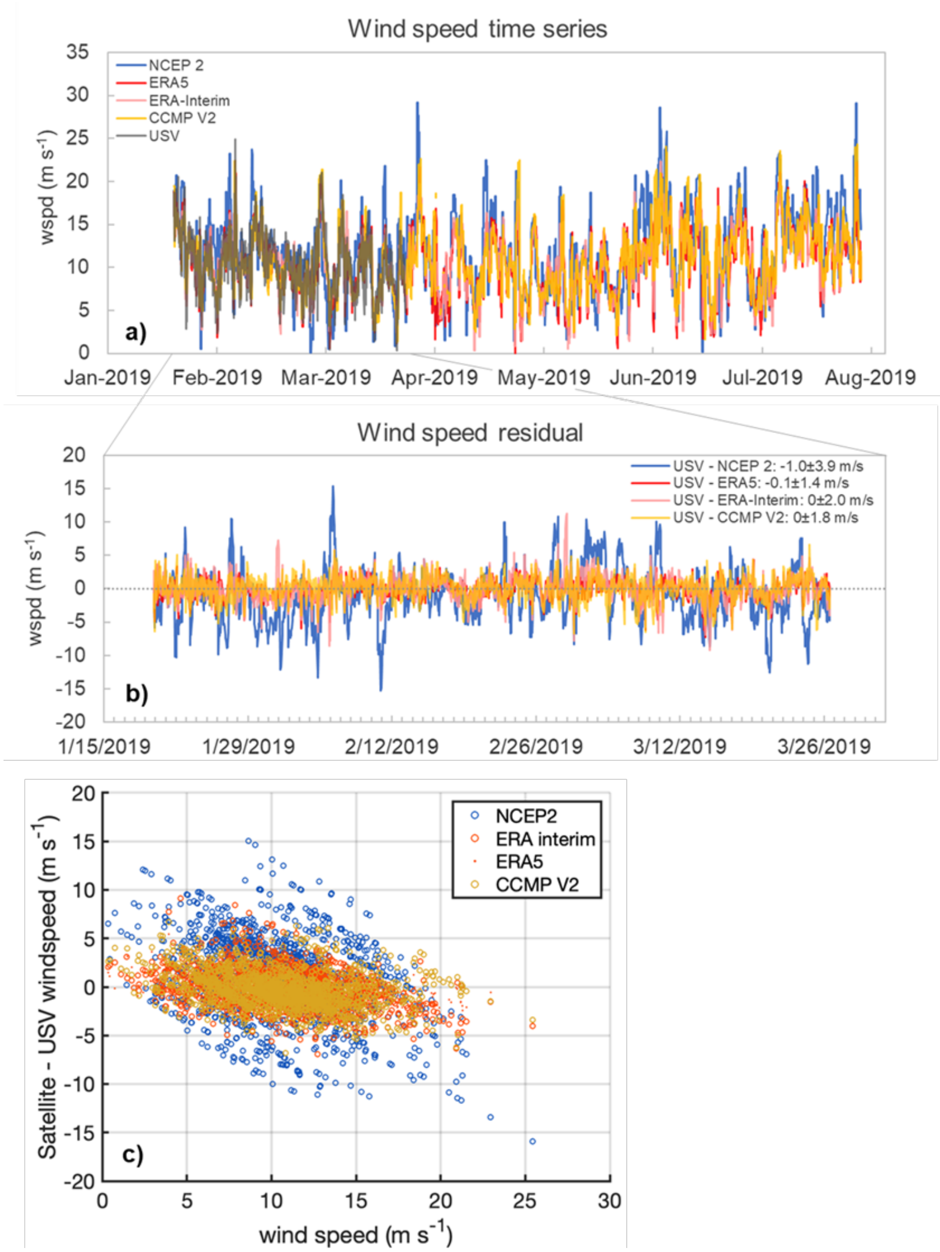

Figure S2. a) Wind speed time series from January to August 2019 from directly-measured Saildrone USV anemometer (gray) and the following satellite-based products: NCEP 2 (dark blue), ERA-Interim Reanalysis (red), ERA5 (pink), and CCMP V2 (yellow). b) Residual between Saildrone-measured wind speed and satellite products (mean residual ± one standard deviation). c) Comparison of wind speed products to USV-measured wind speed as a function of wind speed.

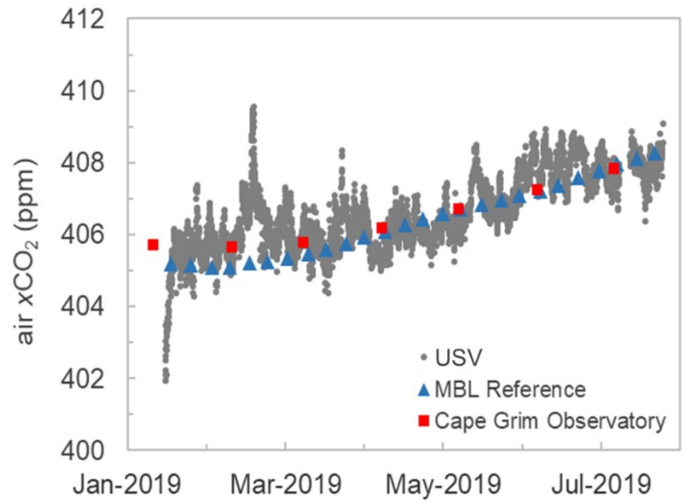

Figure S3. Comparison of directly-measured air xCO_2 (gray), a fixed time series at the Cape Grim Baseline Air Pollution Station (red; data from the Australian Bureau of Meteorology and CSIRO Oceans & Atmosphere), and the NOAA Greenhouse Gas Marine Boundary Layer Reference product (blue; Dlugokencky et al., 2019).

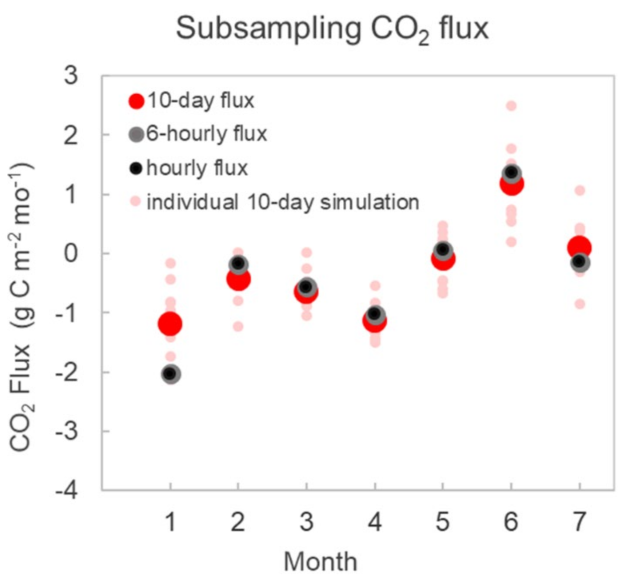

Figure S4. Comparison of calculated monthly mean CO_2 flux using hourly (black), 6-hourly (gray), and 10-day (red) sampling frequencies with each realization of the 10-day subsampling shown in pink.

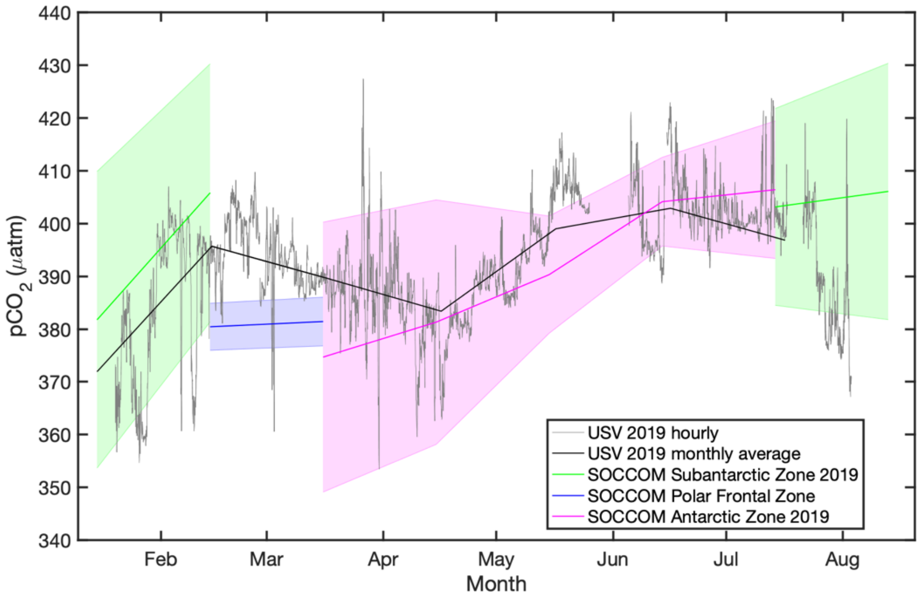

Figure S5. Comparison of hourly and monthly-averaged Saildrone USV directly-measured seawater $p\mathrm{CO}_2$ compared to float-based calculated seawater $p\mathrm{CO}_2$ in the three major Southern Ocean zones sampled during the 2019 Saildrone USV mission. Shaded areas represent 1 σ of monthly mean float-based $p\mathrm{CO}_2$.

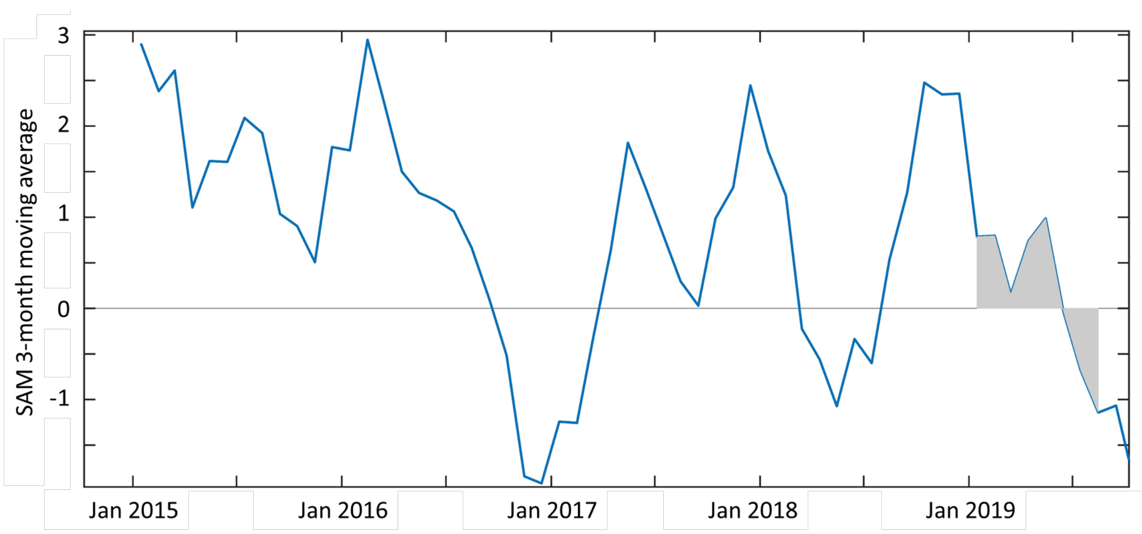

Figure S6. 3-month moving average of the SAM Index based on Marshall (2003). Shaded area is the deployment time for the 2019 Saildrone USV mission.

Source of error	Mean bias	σ
Ship and USV-based pCO_2 (μatm)	-	0.5%
Float-based seawater pCO_2 (μatm)	-	2.8%
NCEP 2 sea level pressure (hPa)	−0.2	3.6
ERA-Interim sea level pressure (hPa)	+0.2	1.8
ERA5 sea level pressure (hPa)	−0.5	0.9
USV wind speed (m s^{-1})	+0.2	1.0
CCMP V2 wind speed (m s^{-1})	+0.2	1.8
NCEP 2 wind speed (m s^{-1})	−0.8	3.9
ERA-Interim wind speed (m s^{-1})	+0.2	2.0
ERA5 wind speed (m s^{-1})	+0.1	1.4
10-day sampling frequency (g C m^{-2} mo^{-1})	+0.05	0.43

Table S1. Sources of error in calculating CO_2 flux from various sources. USV wind speed errors are from Zhang et al (2019). Seawater pCO_2 errors are from previous studies: Pierrot et al. (2009) for ship-based pCO_2, Sabine et al. (2020) for USV-based pCO_2, and Williams et al. (2017) for float-based pCO_2. Mean bias and standard deviation (σ) of sea level atmospheric pressure and wind speed are calculated from residuals between USV-measured parameters and each data product. For wind speed, these biases are reported relative to the "true" wind speed by correcting the difference reported in Figure S2(b) for the USV wind speed bias of +0.2 m s^{-1}. Error due to 10-day sampling frequency of float-based measurements is calculated by subsampling the hourly USV data set at all possible 10-day intervals starting at 12:00 UTC.

	Mean	σ	Range	
air xCO_2 (μmol mol^{-1})	407	1	402	410
seawater pCO_2 (μatm)	393	11	354	427
ΔpCO_2	-4	12	-40	33
SST (°C)	4.8	3.0	-0.3	13.5
SSS	34.04	0.27	32.12	34.95
wind speed (m s^{-1})*	10.2	3.4	0.3	24.9
CCMP-NRT wind speed (m s^{-1})	10.8	3.8	1.3	24.3

* USV wind speed statistics represent measurements made from the beginning of the mission until 26 March 2019 due to loss of sensor. CCMP V2 wind speeds for the entire deployment are also included to indicate that mean, variance, and range during January through March were similar to conditions throughout the deployment.

Table S2. Mean, one standard deviation of the mean (σ), and range of observations measured on the Saildrone USV from 19 January to 3 August 2019.